Figure SI 1: Quantification of photon penetration within spheroids

In optical imaging of thick three-dimensional biological samples, light scattering due to mismatch of refractive index between cellular components limits imaging of deep layers in these samples (Yu et al., 2018). To deal with this issue and to evaluate clarification techniques on enhancement of confocal microscopy of multicellular tumour spheroids, HCT-116 spheroids were prepared via agarose microwells and fixed 72 h after cell seeding. Nuclei were then stained using Nucgreen™ -Dead 488. Two of the samples were incubated in RapiClear or 80%/20% glycerol/PBS solution overnight and the third sample was kept in PBS. All samples were then mounted in iSpacers (2x0.5 mm) with fresh clarification solutions or fresh PBS for control sample. Ten spheroids from each sample were imaged. A qualitative analysis of the images (**Fig. SI 1A**) shows that nuclei fluorescence signal is detected much deeper for clarified spheroids compared to unclarified ones. The orthogonal views of spheroids confirm this (**Fig. SI 1B**). These images were analysed using a routine prepared in Matlab to measure the average fluorescence intensity along the spheroids radius (**Fig. SI 1C**). The mean Intensity of spheroids clarified with glycerol (Green curve) shows the highest mean intensity for all regions in spheroids compared to the two other samples. While the mean intensity of RapiClear-clarified spheroids (Red curve) is lower than glycerol-clarified spheroids in all regions of the spheroids, the intensity decay is similar for both clarified solutions. The 80% glycerol solution was hence selected as the standard clarification technique for all this study.

Yu, T., Zhu, J., Li, Y., Ma, Y., Wang, J., Cheng, X., … Zhu, D. (2018). RTF: A rapid and versatile tissue optical clearing method. *Scientific Reports*, *8*(1), 1–9. https://doi.org/10.1038/s41598-018-20306-3

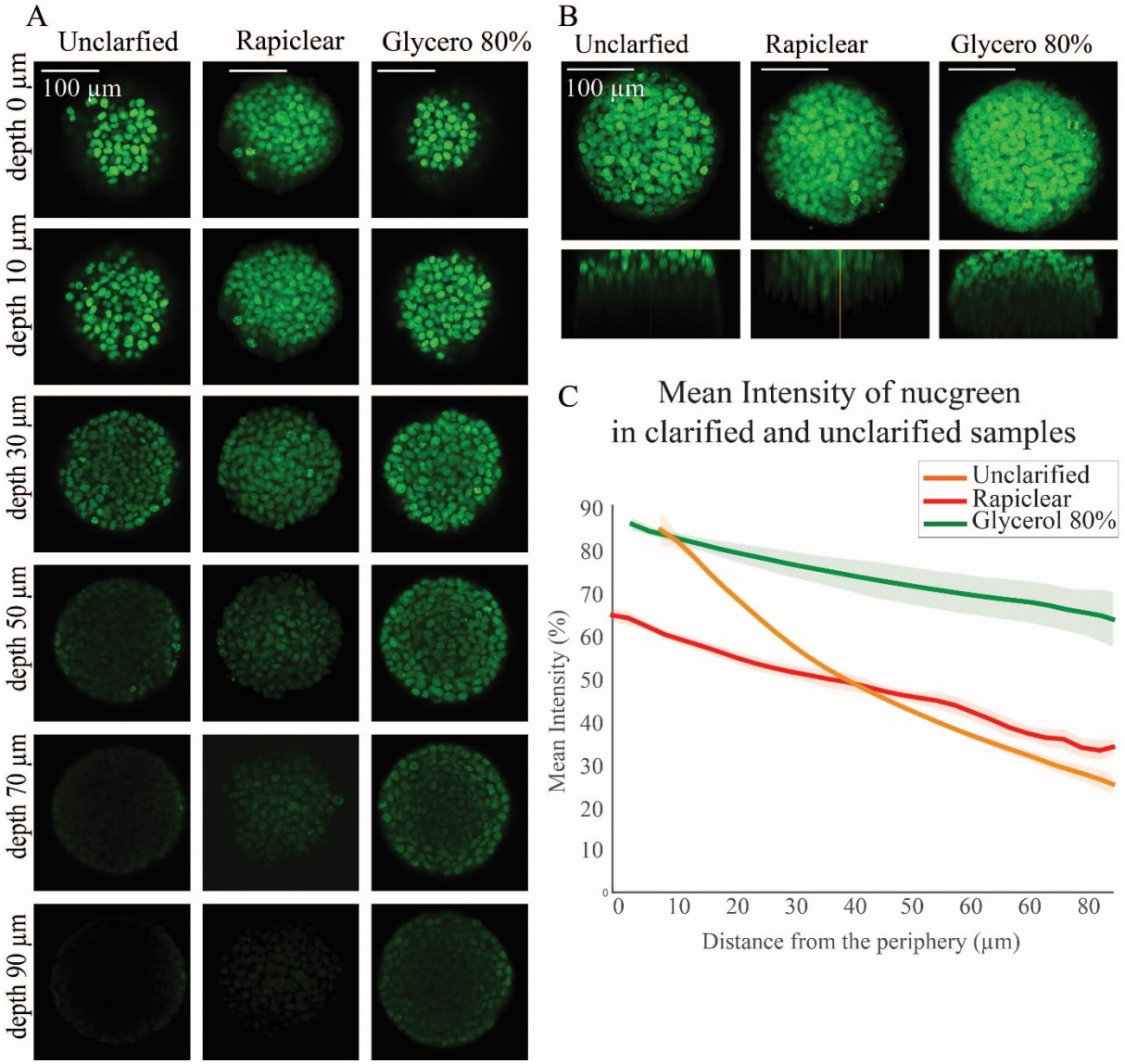

Figure SI 1. Influence of clarification technique on image acquisition and fluorescence signals

(A) *Confocal fluorescence images of HCT-116 cell spheroids labelled with Nucgreen in different depth for unclarified, clarified with Rapiclear and clarified with 80%/20% glycerol/PBS respectively.* ***(B)*** *Maximal Image Projection (MIP) and xz images of clarified and unclarified spheroids.* ***(C)*** *Mean intensity of clarified (green, glycerol-clarification, red, rapiclear-clarification) and unclarified (orange curve) spheroids as a function of the distance from the periphery. Error bars represent standard errors of the Mean (N=10 spheroids for each condition).*

Figure SI 2: Detailed mounting procedure for imaging

There are different possibilities to mount the microwells for optical imaging, depending if one wants to acquire fixed, live spheroids, or to follow spheroids over time using time-lapse.

1-For fixed spheroids, the easiest and quickest way is to mount the microwells between 2 coverslips, separated by a 1 mm sticky spacer (two 0.5 mm-thick iSpacer provided by SunJin Lab were used for their convenience, but other spacers could also be used, **Fig. SI2 B**).

2-For live spheroids, it is possible to transfer the microwells in optical imaging chamber (such as Ibidi® 8-well plate, **Fig. SI2 C**).). We used such possibility in preliminary experiments to check that distribution of nanoparticles were not modified by fixation procedure (data not shown), as well as for the assessment of nanoparticles transport and localization after extensive washing procedure (**Fig. 4**).

3-For time-lapse follow-up, to avoid any drift during acquisition, it is necessary to directly bond the microwells to the coverslips. This is possible using APTS-functionalized coverslips (representation in **Fig. 1D**, patented process[39]). We used such procedure for growth monitoring using time lapse microscopy (**Fig. SI 4**).

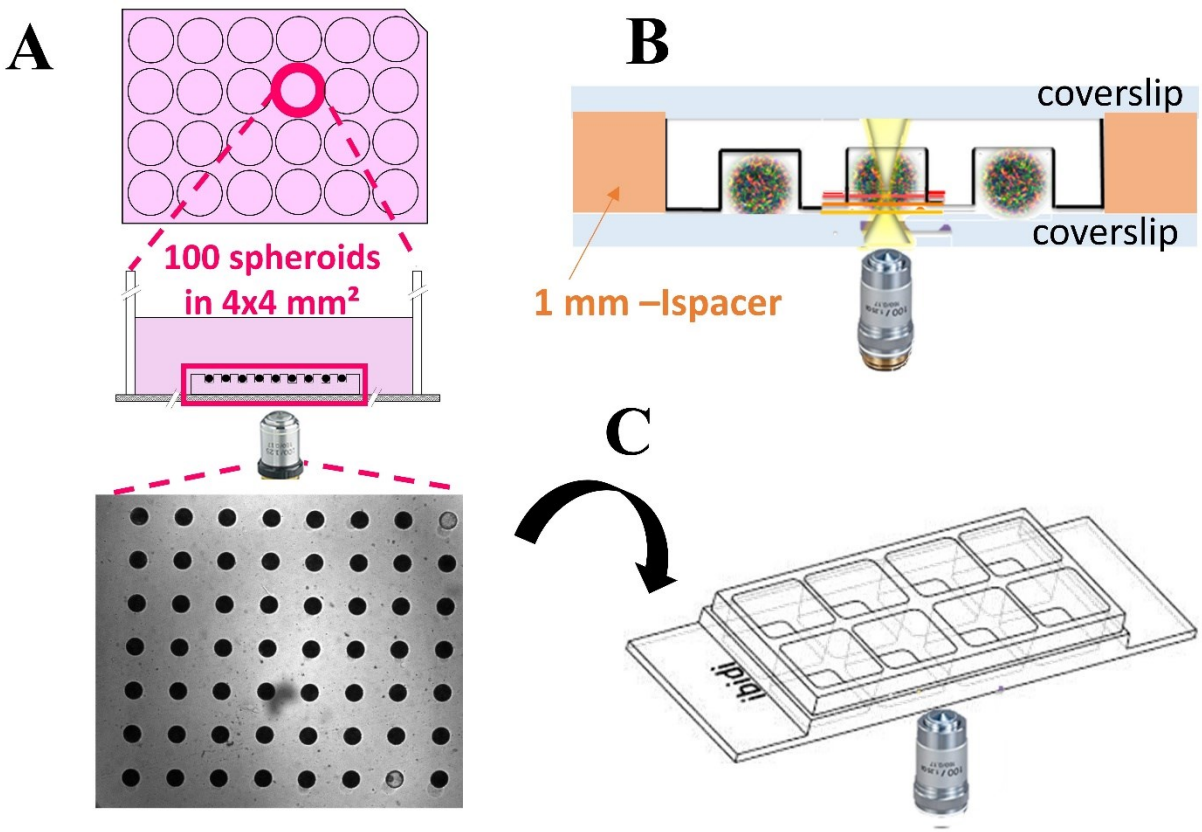

Figure SI 2. Schematic representation of the mounting procedures used for optical imaging

(A) *Schematic representation of free-standing microwells, placed on each well of a multi-well plate.* ***(B)*** *Schematic representation of the mounting used for optical imaging of fixed samples. The agarose microsystems containing the fixed, immunostained and clarified spheroids are mounted between 2 coverslips using a 1 mm sticky spacer (orange-part, Ispacer from SunjinLab).* ***(C)*** *For live imaging of spheroids, it is also possible to transfer the microwells in optical imaging chamber (such as Ibidi® 8-well plates).*

Figure SI 3: Quantification of the removal of FITC and AGuIX®-Cy5.5 nanoparticles in agarose-based microwells

To understand the ability of agarose gel in transporting molecules, the agarose-based microsystems were incubated with either FITC solution (0.05 mM in PBS), either AGuIX®-Cy5.5 nanoparticles (2 mM in complete culture medium). The fluorescent solution was then replaced with PBS (for FITC) or culture medium (for AGuIX®-Cy5.5) and the decrease in fluorescence intensity was followed by time-lapse confocal microscopy. The images of different depths of agarose-based microwells were analysed using a Matlab routine quantifying the mean intensity changes over time (**Fig. SI 3**). For FITC (**Fig.SI3 A**), after the first two hours, there is a 75±5% reduction in the initial mean intensity in the microsystem, reaching a plateau at 25±5 % depending on the depth of the focal plane. All curves were exponentially decreasing with a characteristic time of 25 min (23-27 min depending on the depth of the focal plane).

As expected, as AGuiX®-Cy5.5 nanoparticles (D_H=5 nm) are much larger than FITC (Mw=376 g/mol, D_H~0,25 nm), the diffusion is one order of magnitude slower than with FITC, but still efficient in the agarose, both when culture medium is replaced by AGuIX®-Cy5.5 (**Fig.SI3 B)**, or when AGuIX®-Cy5.5 is replaced by culture medium (**Fig.SI3 C).** When culture medium is replaced by AGuIX®-Cy5.5, the characteristic time obtained for the deepest part of the gel is of the order of 22-24 min (23,9 ±0.4 min for Z=0, 23,6 ±0.6 min for Z=80 µm and 22,4 ±1,7 min for Z=160 µm), while it already reached the maximum intensity upon imaging for the upper part (z=240 µm). When AGuIX®-Cy5.5 is replaced by culture medium (after 3x15 min washing, following the procedure done for all experiments), the fluorescent is decreasing with a characteristic time of the order of 1-2h, depending of the depth (69 ±5 min for Z=0, 82±6 min for Z=80 µm, 104 ±5 min for Z=160 µm and 129 ±5 min for Z=240 µm).

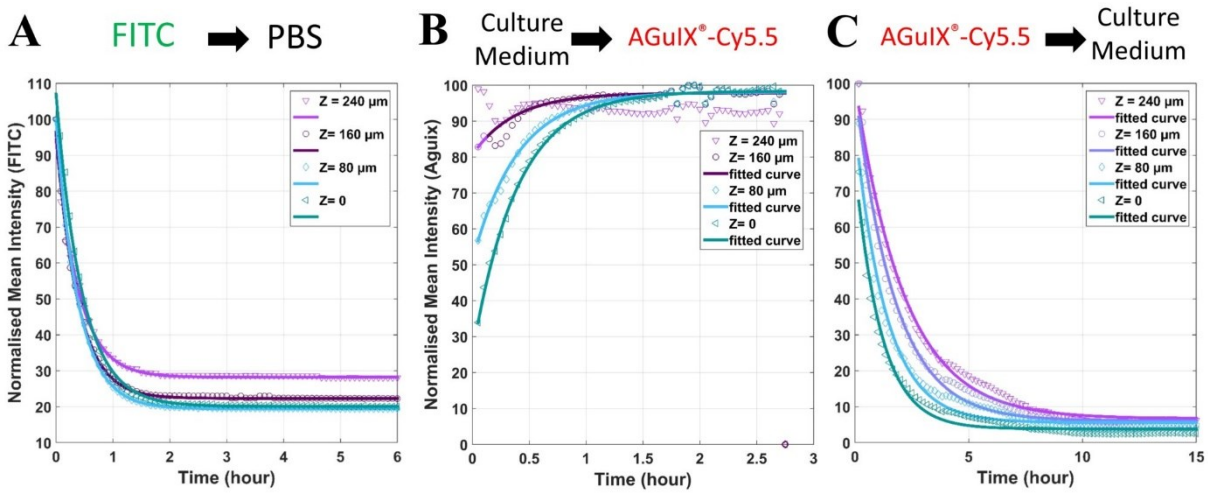

Figure SI 3.

(A) *Reduction in fluorescence intensity of FITC dye in an agarose microsystem over time for different depth (from Z=0, corresponding to the depth closest to the objective and farthest from the solution reservoir to Z=240 µm, farthest from the objective and closest to solution reservoir). Experimental points are plotted with different markers (Z=0, (pink triangles pointing down), Z=80 µm (blue diamonds), Z=160 µm (purple circles), Z=240 µm (green triangles pointing left)) and the corresponding exponential fit are plotted in bold lines [fitting model a*exp(-time/T)+b].*

(B) *Increase in fluorescence intensity of AGuIX®-Cy5.5 nanoparticles in an agarose microsystem over time for different depth (same legend than in (A)). [fitting model a*(1-exp(-time/T))+c].*

(C) *Reduction in fluorescence intensity of AGuIX®-Cy5.5 nanoparticles in an agarose microsystem over time for different depth (same legend than in (A). [fitting model a*exp(-time/T)+b].*

Figure SI 4. Time-lapse follow-up of spheroid growth

To understand the influence of AGuIX®-Cy5.5. nanoparticles on the cell proliferation and growth rate of HCT-116 cell spheroids, cells were seeded in agarose-based microwells using APTS-functionnalised coverslips. This procedure enables live imaging with no drift of the microwells over-time. After 48 h, the HCT-116 spheroids were exposed to AGuIX®-Cy5.5 nanoparticles with three different concentrations (0.8, 1.5 and 2 mM). Control samples with no AGuIX®-Cy5.5 nanoparticles were also monitored in parallel. The growth of spheroids was followed by time-lapse optical microscopy during three days of incubation with AGuIX®-Cy5.5 nanoparticles (time interval between each image acquisition = 4 h). These images were manually segmented using a dedicated routine in Matlab. Then, from the projected area, an equivalent diameter was computed, and making the assumption of spherical shape, the equivalent volume of each spheroids was calculated. Spheroids growth is followed by representing the relative evolution of the volume over time (Volume normalised by the initial volume [at day 2]).

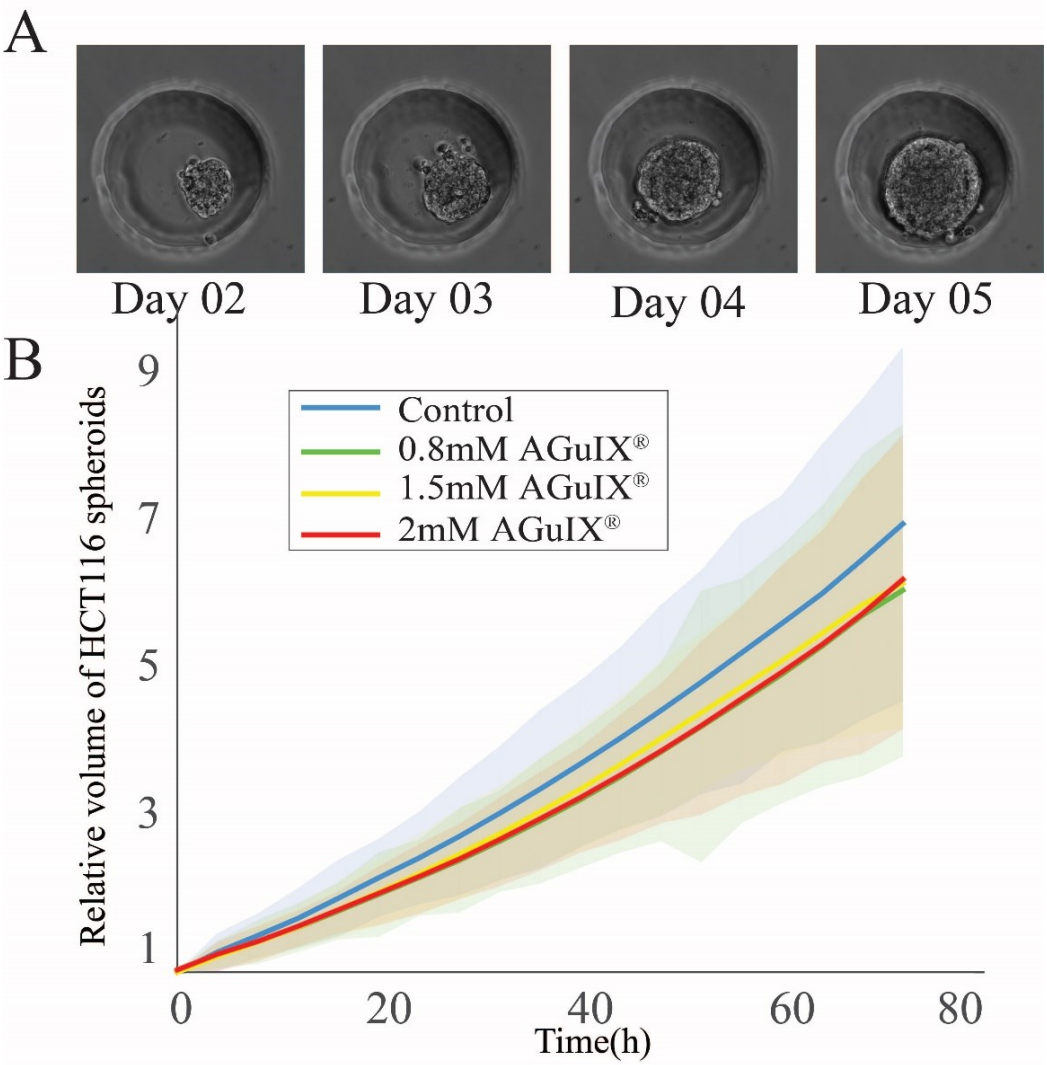

Figure SI 4. ***Follow-up of spheroids growth via optical time-lapse microscopy.***

(A) *Representative images of daily growth of control HCT-116 spheroids from day 2 to day 5. The well is 200 µm in diameter.* ***(B)*** *Evolution of the relative volume of spheroids as a function of time for control sample and in the presence of three different concentrations of AGuIX®-Cy5.5 nanoparticles. Bold lines represent the mean values, and light area represents the standard*

deviation for each condition (control –blue- [N=102 spheroids], 0.8mM –green-[N=89 spheroids], 1.5mM –yellow-[N=88 spheroids], 2mM –red-[N=102 spheroids]). Three independent experiments for each condition.

Figure SI 5. Characterization of spheroids size distribution from Day 2 to Day 4 after cell seeding

One advantage of using agarose-based microwells to prepare multicellular tumour spheroids is the homogeneity of spheroids size. To show the homogeneity of spheroids, the equivalent diameter for each spheroid was calculated during the growth follow-up **(Fig. SI 4)**. From this, the distribution of spheroids diameter in day 2, day 3 and day 4 for control conditions were plotted using the UnivarScatter matlab function developed by Manuel Lera Ramírez (Copyright (c) 2015).

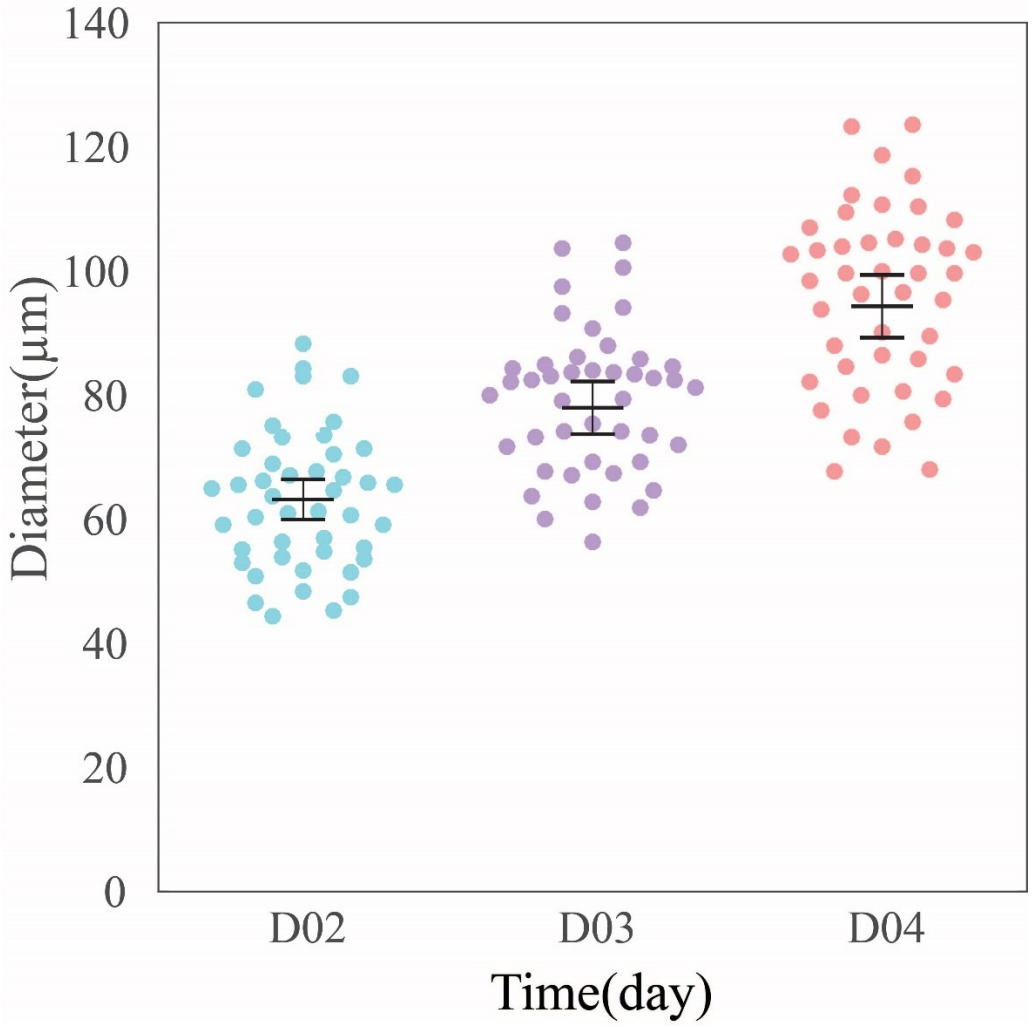

Figure SI 5.

Distribution of HCT-116 multicellular tumour spheroids at day two (blue circles), day three (purple circle) and day four (orange circles) after cell seeding in the agarose-based microwells. Mean values and 95 % Standard Error of the Mean are represented.

Figure SI 6. Importance of statistics

Due to cell heterogeneity, large statistical variances are expected, even if our process enables to generate very reproducible spheroids in terms of size. The variance on the Mean Intensity of the fluorescence signal of AGuIX®-Cy5.5 nanoparticles is analysed in **Fig.SI 6**, for different distance from the periphery.

The standard deviation of the normalized Intensity of AGuIX®-Cy5.5 obtained, is calculated as a function of the number (N) of spheroids, with a random sampling of N spheroids over the 121 spheroids acquired for this experimental condition (24h incubation with 2mM AGuIX®-Cy5.5). The random sampling is repeated 10 times to simulate 10 different experiments, and the mean of the obtained SD computed. The obtained SD first increases, until reaching a plateau around N=20-40 spheroids (**Fig. SI6, Inset**). The initial rising may be attributed to the heterogeneity among spheroids.

The plateau of the SD is increasing with the distance from the periphery (with a plateau at ~5% for 30 and 50 µm from the periphery, and up to ~10% for 80 µm from the periphery).

Once the plateau is reached, the standard error of the mean (SEM) and the relative standard errors (RSE=SEM/mean) on the normalized Intensity are therefore decreasing with N as $N^{-1/2}$ (**Fig. SI 6**). To get a RSE below 2%, N=20-25 spheroids are necessary for an analysis up to 60 µm from the periphery. For deep layers, a larger number of spheroids are needed to reach such RSE (N=70 spheroids for 80 µm from the periphery). Hence a minimum of N=30 spheroids is recommended to get reliable results at an imaging depth corresponding to the first quarter of the spheroids. This number rises up to N=70 spheroids for an accurate analysis close to the equatorial plane.

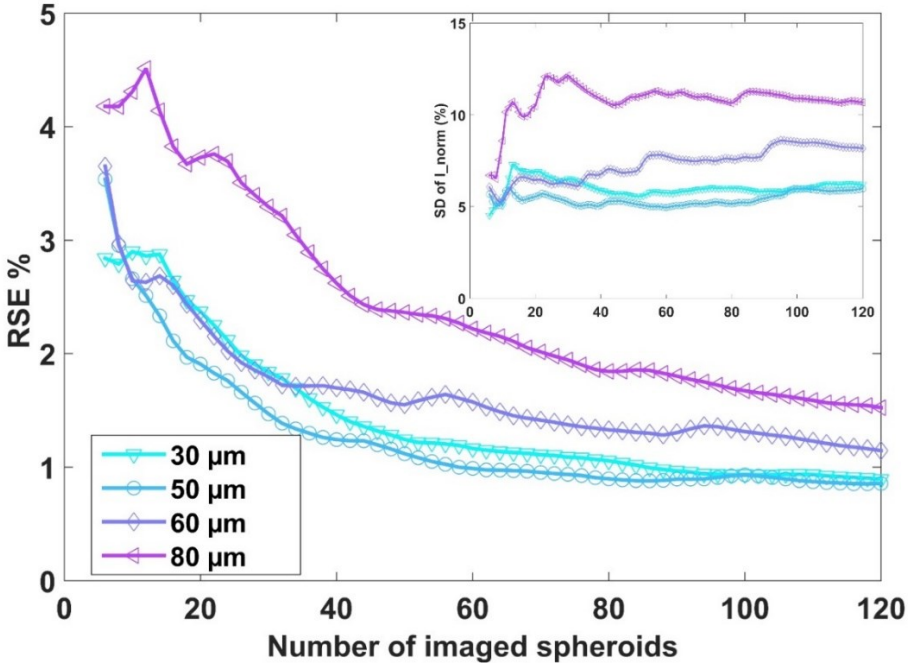

Figure SI 6. Error analysis due to the number of spheroids analysed.

Relative Standard Error (RSE=SEM/mean) as a function of the number of spheroids for different distance from the periphery (30 µm (cyan, triangles pointing down), 50 µm (light blue, circles), 60 µm (intense blue, diamonds) and 80 µm (purple, triangles pointing left). ***Inset:*** *Standard Deviation (SD) of the normalised Intensity I_norm as a function of the number of spheroids, for the same distance from the periphery.*

Figure SI 7. Control experiments using Ultra-Low Adhesion multi-well plate

The goal of this experiment was to compare the distribution of AGuIX®-Cy5.5 nanoparticles in HCT-116 spheroids prepared in a traditional ultra-low adhesion 96-well plate with spheroids made in agarose microwells. HCT-116 cells were seeded at a density of 10 cells/well in a 96-well plate (200 µl culture medium per well), and spheroids were formed through self-assembly aggregation. During culture, the plate was on the agitator. Spheroids were exposed to 2 mM AGuIX®-Cy5.5 nanoparticles at day 3. To avoid losing spheroids, half of the medium was withdrawn and 100 µl of AGuIX®-Cy5.5 nanoparticles at a concentration of 4mM were added in each well to have a final concentration of 2mM. After 24 h, spheroids were rinsed with fresh medium (3X, 15 min), fixed with PFA 4%, permeabilized with PBS/0.1% Triton-X, and blocked with PBS/2% BSA/0.1% Triton-X. The spheroids were then labelled with nucgreen™ at a dilution of 1 drop/ 2 ml for overnight at room temperature before being rinsed with PBS (3X, 5 min).

Spheroids could not be imaged in a standard 96-well plate using confocal microscopy; thus they were transferred to an ibidi 96-well plate and imaged.

The same Matlab routine that was used to analyse images of spheroids in microwells was used to analyse these images. Despite the fact that the number of imaged spheroids in this experiment is considerably lower than spheroids in microwells which is due to the limitations of different steps of experiments using a standard 96-well plate, the analysed results show that the distribution and amount of uptaken nanoparticles are similar to spheroids in microwells. This finding supports the permeability of agarose gels for AGuIX®-Cy5.5 nanoparticles and validates the usage of such microsystems for spheroids generation and high-throughput drug screening in a more practicable and reproducible manner.

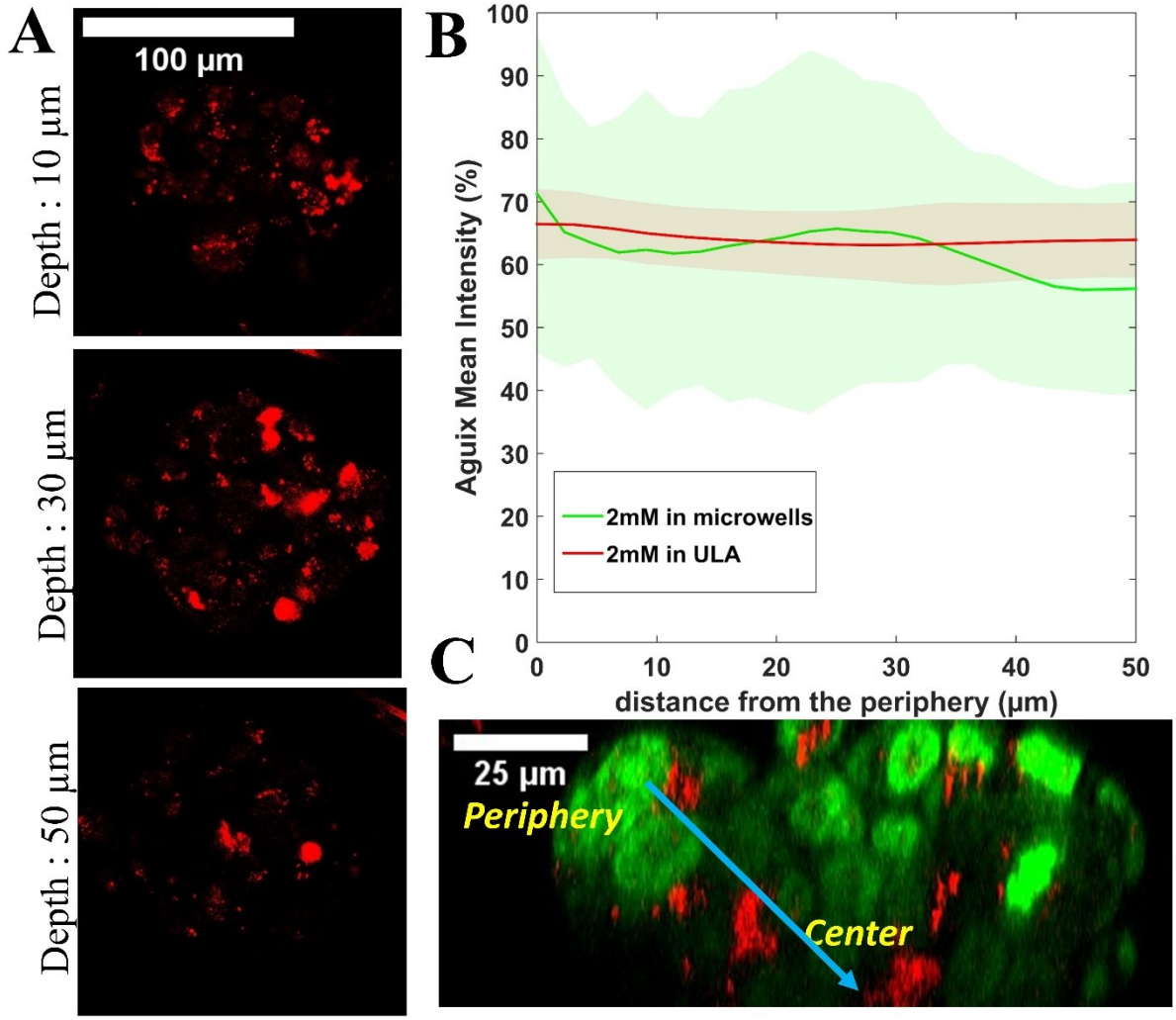

Figure SI 7. Control experiments using Ultra-Low Adhesion (ULA)multi-well plate

(A) Representative confocal fluorescence images of HCT-116 spheroids grown in Ultra-Low-Adhesion multi-well plates for 4 days, then incubated with 2 mM concentration of AGuIX®-Cy5.5 for 24 h for three different depths (10, 30 and 50 µm). **(B)** Mean intensity of AGuIX®-Cy 5.5 after 24h incubation with 2 mM AGuIX®-Cy5.5 as a function of the distance from the periphery in our microsystems (red, N=121, three independent experiment), and in ULA multi-well plates (green, N=10, one experiment). Standard deviations are shown in light colors. **(C)** Orthogonal view of the spheroid in (A) (green=nuclei, red = AGuIX®-Cy5.5).

Figure SI 8. HCT-116 cell incubated in 2D with nanoparticles and spheroid formation afterwards

To make a comparison between cellular uptake of AGuIX®-Cy5.5 nanoparticles in monolayer cells and multicellular tumour spheroids, two parallel experiments have been done.

In the first experiment, HCT-116 cells were seeded in agarose-based microwells (**Fig. SI 8A A, Step I**) and after 48 h were exposed to AGuIX®-Cy5.5 nanoparticles for 24h (**Fig. SI 8A, Step II**) followed by fixation (**Fig. SI 8A, Step III**).

In the other experiment HCT-116 monolayer cells that were first exposed to AGuIX®-Cy5.5 nanoparticles for 24 h (**Fig. SI 8B, Step I**), and then seeded in agarose-based microwells to allow spheroid formation (**Fig. SI 8B, Step II**). After 72h, these spheroids were fixed (**Fig. SI 8B, Step III**).

Spheroids from both experiments were clarified with glycerol 80% (**Fig. SI 8, Step III**) and imaged via confocal microscopy. The confocal images of these two experiments and orthogonal view of spheroids demonstrate that when spheroids are incubated with nanoparticles, clusters could be observed evenly in extracellular and intracellular regions of spheroids and nanoparticles clusters are more in peripheral region than in the centre (**Fig. SI 8A**). When spheroids are made from already AGuIX®-Cy5.5 labelled cells, only sparse clusters, with a scattered distribution are observed in spheroids (**Fig. SI 8B)**.

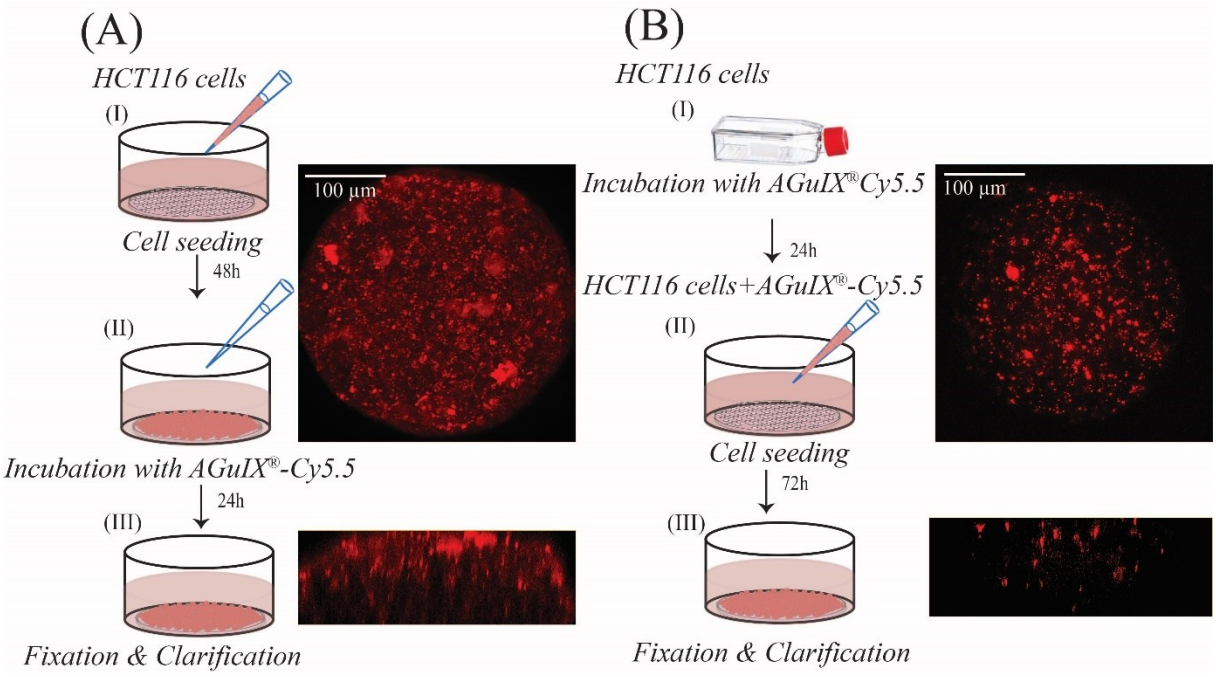

Figure SI. 8. ***Difference in distribution of AGuIX®-Cy 5.5 nanoparticles in HCT116 multicellular tumour spheroids incubated in 2D and 3D cell culture.***

*(A) Spheroids were prepared with agarose-based microwells (**Step I**). After 48 h, they were exposed to 2mM AGuIX®-Cy5.5 nanoparticles for 24h **(step II)** and were fixed, clarified **(Step III)** and imaged with confocal microscopy. (B) Monolayer HCT116 cells were first incubated with 2mM AGuIX® nanoparticles for 24h **(Step I)** and then HCT116 spheroids were prepared with these cells **(step II)**. Spheroids were fixed, clarified **(Step III)** and imaged with confocal microscopy.*

Figure SI 9. Nanoscale Secondary Ion Mass Spectrometry control analysis

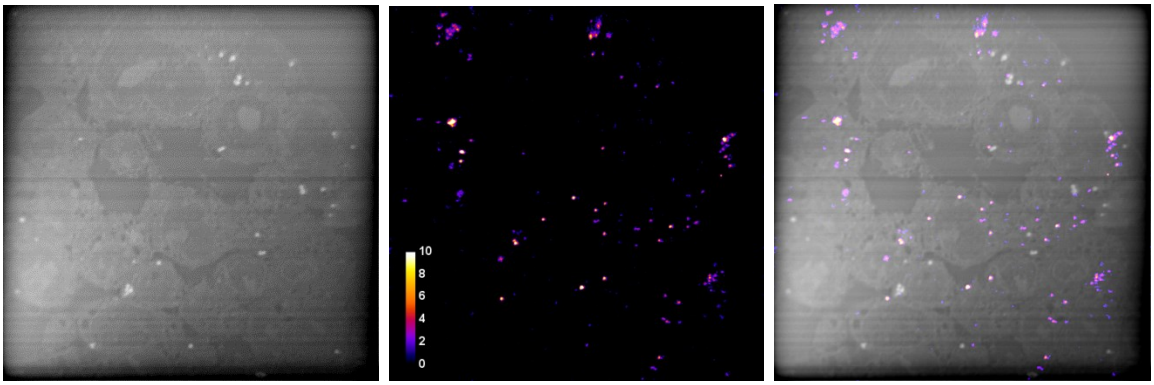

Figure SI. 9.

(A) *NanoSIMS image of $^{12}C^-$ of the same area as in* ***Figure 5*** *provides the proof of the entirety of the section. The slight contrast is due to the compositional variation of different cells compartments and the surrounding resin (the actual contrast is much lower). A few spots with unusually high $^{12}C^-$ emission are probably location of vacuoles.* ***(B)*** *Recalled of the distribution of AGuIX®-Cy5.5 nanoparticles.* ***(C)*** *Merged image of $^{28}Si^-$ and $^{12}C^-$. Image field: 60 µm.*

Figure SI 10. Localization of AGuIX-Cy5.5-nanoparticles after an extensive washing procedure

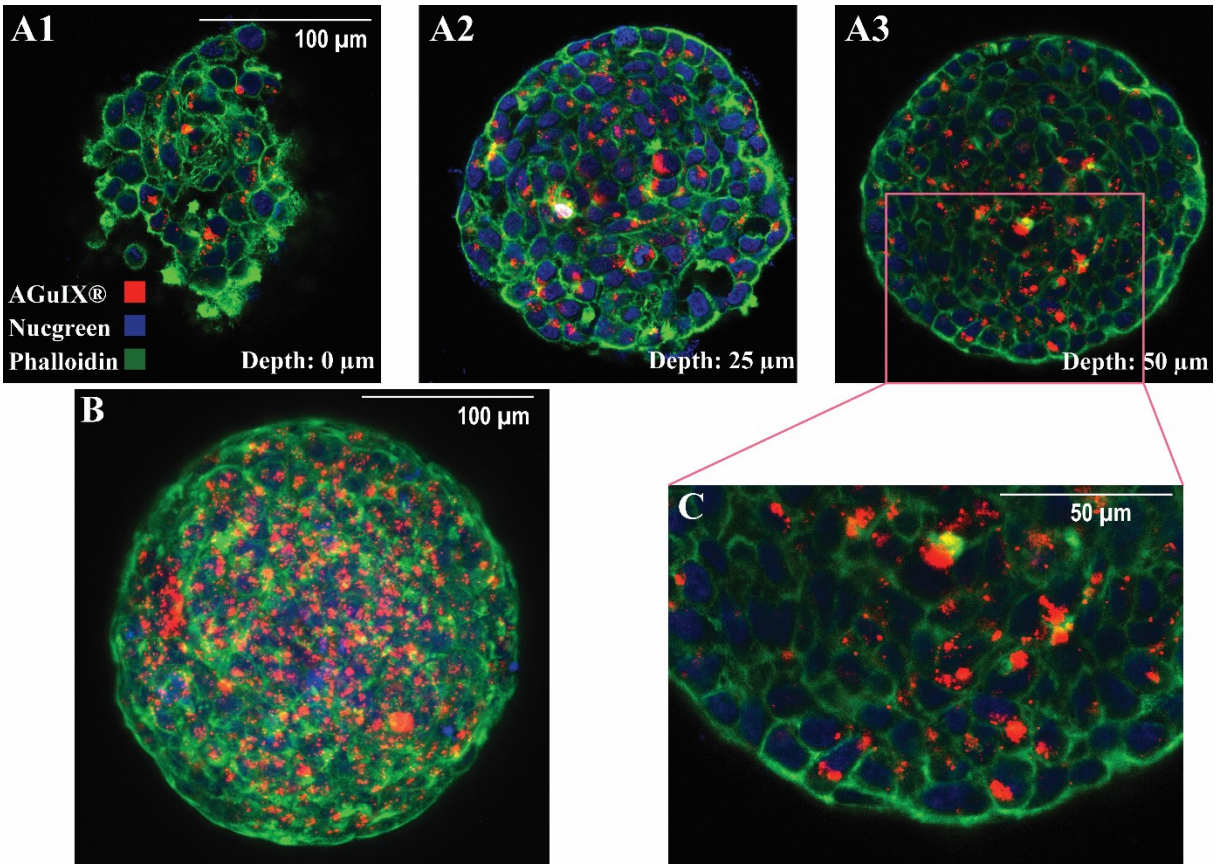

Figure SI. 10. ***Localization of Aguix-Cy5.5-nanoparticles after an extensive washing procedure within HCT-116 spheroids***

Confocal fluorescence images of HCT-116 spheroids incubated with AGuIX®-Cy5.5 nanoparticles for 72 h with 2 mM AGuIX®-Cy5.5 solution, and washed according to the procedure mentioned in Figure 4, then fixed and immunostained with antibodies to find colocalization of nanoparticles in spheroids. For all images, red, blue and green channels are staining AGuIX®-Cy5.5, nuclei and phalloidin (Actins) respectively.

(A1-A3) *Representative images of phalloidin immunostaining merged with AGuIX®-Cy5.5 and Nucgreen layers obtained at various depths (**A1-0µm, A2-25 µm, A3-50µm**).* ***(B)*** *Maximal Image Projection (MIP) of confocal fluorescence image of spheroid in (A1-A3).* ***(C)*** *Zoomed-in portion of merged image at a depth of 50 µm (square in A3).*